Polymer Chemistry

ROYAL SOCIETY OF CHEMISTRY

PAPER

View Article Online
View Journal | View Issue

Cite this: *Polym. Chem.*, 2022, **13**, 3790

Morphological transitions of cationic PISA particles by salt, triflate ions and temperature; comparison of three polycations†

Vikram Baddam, Lauri Välinen, Linus Kuckling and Heikki Tenhu *

Three strong polycation stabilizers, poly((vinylbenzyl) trimethylammonium chloride), PVBTMAC, poly((2-(methacryloyloxy)ethyl)trimethylammonium chloride), PMOTAC, and poly((3-acrylamidopropyl) trimethylammonium chloride), PAMPTMAC have been synthesized with reversible addition–fragmentation chain transfer, RAFT, reactions. Solubilities of the polycations change with hydrophobic counterions such as triflate. PVBTMAC undergoes a thermal phase transition with a low amount of triflate, whereas PMOTAC or PAMPTMAC do not. These three cationic macro chain transfer agents were chain extended with a hydrophobic core forming monomer diacetone acrylamide, DAAM, in polymerization-induced self-assembly (PISA) processes. In aqueous sodium chloride solutions, the obtained particles show morphological transitions from spheres to aggregated structures and to vesicles with increasing the ionic ratio (salt concentration). With either increasing the DP of the PVBTMAC block or using other polycations, the particle morphologies change to raspberry-like ones at high salt or solids concentration. When PVBTMACs were used as stabilizers in aqueous LiOTf dispersions at elevated temperatures, spherical particles fused together. Upon cooling, the particles either aggregated or formed worm-like structures. On the other hand, no morphological changes were observed when other two polycations were used as CTAs. The results show how changes in the chemical structure and hydrophilicity of the polycation affect the morphologies of the particles. Particle morphologies may be further tuned with hydrophobic counterions, with which also thermoresponsive morphological changes can be induced.

Received 9th March 2022,
Accepted 6th June 2022

DOI: 10.1039/d2py00301e

rsc.li/polymers

Introduction

Polymerization induced self-assembly (PISA) is a much studied method for synthesizing block copolymer nanoparticles with various morphologies. During the polymerization, the growing block copolymers assemble into spheres, worms and vesicles. The final morphology of the nanoparticles depends on several parameters like, *e.g.*, mole fractions of hydrophilic and hydrophobic chains, solids content, pH, solvent, and ionic strength.[1–16]

Often block copolymers self-assemble to kinetically trapped spheres in PISA, due to either steric hindrance by the long stabilizer blocks or charge repulsions of polyelectrolyte stabilizers.[7,17–19] Several strong polycations *e.g.* imidazolium containing ones and especially quaternary ammonium salts, have been chain extended with core forming methacrylate/acrylate monomers in PISA.[20–26] In most of the cases, the copolymer morphology was limited to only spheres due to high charge density in the corona. However, diluting the charges by using non-ionic co-stabilizers in aqueous systems leads to a morphological transition from spheres to worms or vesicles. This has been well demonstrated for a few (meth)acrylate based polyelectrolytes with or without salt.[20,22]

Under certain conditions, the particles obtained through PISA can undergo morphological transitions when the copolymers respond to external stimuli and/or due to the surface plasticization of the core forming blocks. For example, several aqueous PISA systems with partially hydrophilic poly(2-hydroxypropyl methacrylate) (PHPMA) as a core forming block show thermally induced morphological transitions.[27–33] Due to the hydration changes of the PHPMA block segments, the morphological transformation takes place from vesicles or worms to spheres upon cooling to 4 °C or below.[27,34–36] Poly(glycerol monomethacrylate)-poly(2-hydroxypropyl methacrylate) (PGMA-PHPMA) diblock copolymers carrying carboxylic groups in the end of the hydrophilic block undergo order–order transitions with changing the pH, due to the protonation of the acid end groups.[29,37] Poly (diacetone acryl-

Department of Chemistry, PB 55, University of Helsinki, Helsinki FIN-00014, Finland. E-mail: heikki.tenhu@helsinki.fi

†Electronic supplementary information (ESI) available: Characterization methods, ^{1}H NMR spectra of polycation macroCTAs and diblock copolymers, lists of the syntheses of nanoparticles, TEM images of the particles, DLS size distributions of the particles obtained from LiOTf series at 15 w/w%. See DOI: https://doi.org/10.1039/d2py00301e

amide) (PDAAM) is another example of a core-forming block in aqueous PISA. Morphological transitions from spheres to worms and vesicles or lamella have been observed for the copolymers of PDAAM. However, the transitions are rather weak to stimulus changes and depend on the core composition.[38–40]

In contrast to aqueous PISA systems, particles of poly(stearyl methacrylate)-poly(benzyl methacrylate) (PSMA-PBzMA) block copolymers in mineral oil undergo vesicles to worm to spherical/sphere transition upon heating.[41,42] The diblock copolymer worms prepared by chain extension of poly[2-(dimethylamino) ethyl methacrylate]s with 3-phenylpropyl methacrylate *via* RAFT dispersion polymerization in ethanol show changes in morphologies from worms to spheres upon heating to 70 °C.[43] Temperature induced morphological transitions in the non-aqueous systems are rapid compared to the aqueous ones discussed above.

It has been shown that aqueous polycations may be turned into thermoresponsive polymers, and they can undergo either UCST or LCST type phase transitions. The type of the thermal transition depends on the details of the structure of the cationic unit, but also on the counter ion.[44–50] Together with bulky counter ions, styrene-based polycations are relatively hydrophobic and thus, they undergo a thermal phase transition easier than more hydrophilic (meth)acrylate-based polycations.[44,51] We have recently shown that using styrene based polycations as sole stabilizer blocks in PISA, one can produce a full window of morphologies by adjusting the ionic strength in the reactions.[52] In addition, the self-assembled nanostructures can be turned to thermoresponsive ones with addition of triflate (OTf^-) ions.

Herein, we widen the scope of our studies on cationic block copolymers in PISA. First, styrene-based polycation macroCTAs (PVBTMAC) with three different degrees of polymerizations were chain extended with DAAM in aqueous salt solutions to construct a full morphological phase diagram. The particle morphologies were then compared with those obtained from two other copolymers of DAAM. Thus, two polycations, poly((2-(methacryloyloxy)ethyl)trimethylammonium chloride) (PMOTAC) and poly((3-acrylamidopropyl)trimethylammonium chloride) (PAMPTMAC) were chain extended with DAAM. In addition, we also used triflate counterions in the PISA reactions. Because the solubilities of the polycations change in the presence of triflate ions, by using relatively small amounts of triflate in the PISA reactions may be expected to induce higher-order morphologies at elevated temperature. This approach should also enable morphological transitions with changing temperature. No reports exist on morphological transitions triggered by hydrophobic counter ions in aqueous PISA systems where polycations are used as stabilizers.

Experimental part

Materials

(Vinylbenzyl)trimethylammonium chloride (VBTMAC; 99%), (3-acrylamidopropyl)trimethylammonium chloride (AMPTMAC; 75 wt% in H_2O), [2-(methacryloyloxy)ethyl]trimethylammonium chloride (MOTAC; 75 wt% in H_2O), diacetone acrylamide (DAAM; 99%), 2-(2-carboxyethylsulfanylthiocarbonylsulfanyl) propionic acid (CTPA; 95%), 4-((((2-carboxyethyl)thio)carbonothioyl)thio)-4-cyanopentanoic acid (CCTPA) (95%) and 4,4′-azobis(4-cyanovaleric acid) (ACVA; ≥75%) were received from Sigma Aldrich. Sodium chloride (NaCl) was from Fisher Scientific (≥99.0%). Lithium trifluoromethanesulfoate (LiOTf; 99.995%) and methanol (HPLC grade, ≥99.9%) were from Sigma Aldrich. Deionized water was from ELGA pure lab ultra-purification system. Regenerated cellulose membrane tubes (MCWO of 1 kDa) from Spectrumlabs were used in dialysis. All deuterated solvents were purchased from Eurisotop (Cambridge Isotope Laboratories, UK).

Syntheses of polycation macroCTAs

The polycation stabilizers were synthesized *via* RAFT solution polymerization. The chain transfer agent, CTPA, was used in the polymerization of both VBTMAC and APMTMAC. For PMOTAC macroCTA, another suitable chain transfer agent, CCTPA, was used.

For instance, the procedure for the synthesis of the $PVBTMAC_{50}$ macro-chain transfer agent (macroCTA) was as follows. In a reaction flask, the reagents 1.93 g (9.142 mmol) of VBTMAC, 38.77 mg (0.152 mmol) of CTPA and 7.16 mg (0.025 mmol) of ACVA as initiator were mixed in 11 ml of water. Then the reaction mixture was purged with inert gas for 45 min prior to the flask was transferred to a preheated oil bath at 70 °C. After 3.5 h, the reaction was quenched by liquid N_2. The crude polymer was purified by dialysis for two or three days and then collected by freeze-drying. The reaction aliquots were characterized with NMR and SEC for the monomer conversion. The same protocol was applied for the syntheses of other macroCTAs. Reaction conditions and molar masses of the macroCTAs are reported in Table 1.

Synthesis of diblock copolymers *via* aqueous RAFT dispersion polymerization

RAFT dispersion polymerizations of DAAM were conducted with different polycation macroCTAs. In the first series, the polymerizations were conducted with targeting a constant DP of PDAAM and changing the parameters such as NaCl concentration (see Table S1†) and solids content (see Table S2†). In the latter series, all polycation macroCTAs were chain extended with DAAM in aqueous triflate solutions with varying the LiOTf and solids contents (Table S3†).

All the polymerizations of DAAM were conducted in a similar fashion. First, stock solutions of the reagents were prepared in aqueous medium. Then, required amounts were transferred to the reaction vials and purged with N_2 gas for ~25 min. The polymerizations were conducted at 70 °C for 3–4 h. The dispersions obtained from all series were characterized by NMR, DLS and TEM, see ESI.†

Table 1 List of polycation macroCTAs synthesized *via* RAFT polymerization

Entry	[M] : [CTA] : [I]	CTA	Conversion (%)	$M_{n\ (theo)}$ [a] (g mol^{-1})	$M_{n\ (NMR)}$ [b] (g mol^{-1})	$DP_{(NMR)}$ [b]	$M_{n\ (SEC)}$ [c]	$PDI_{(SEC)}$ [c]
$PVBTMAC_{24}$	30 : 1 : 0.2	CPA	86	5700	5330	24	5100	1.27
$PVBTMAC_{50}$	60 : 1 : 0.16	CPA	87	11 300	10 900	50	8747	1.30
$PVBTMAC_{61}$	85 : 1 : 0.1	CPA	77	14 100	13 100	61	10 549	1.36
$PAMPTMAC_{29}$	30 : 1 : 0.1	CPA	91	5900	6300	29	6225	1.30
$PMOTAC_{24}$	30 : 1 : 0.2	CCPA	96	6300	5300	24	5767	1.34

[a] Theoretical M_n was calculated from the equation $M_n = \frac{[M]}{[CTA]} \times conv.\% \times M_{monomer} + M_{CTA}$. [b] M_n and DP were calculated from NMR by end group analysis $M_n = DP \times M_{monomer} + M_{CTA}$. [c] M_n and PDI were collected from size exclusion chromatography.

Results and discussion

Polycation macroCTAs

Three chemically different (styrene, acrylamide, methacrylate) quaternary ammonium chloride macroCTAs were synthesized *via* RAFT polymerization (Scheme 1). In addition, two more styrenic ones with different molar masses were prepared. Two different CTAs were used. Styrene and acrylamide derivatives were synthesized as described earlier.[48] CPA does not work with the methacrylate monomer, however, and in that case we switched to CCPA.

The degrees of polymerization and molar masses of the pure polymers were determined with NMR and SEC, see Table 1. In the NMR analysis, methyl proton peaks (3H, $-CH_3$ around 1 ppm) from CPA were used as a reference to determine the final DP of PVBTMAC and PAMPTMAC macroCTAs. In the case of PMOTAC macroCTA the proton peak at 2.25 ppm from CCPA was used to calculate the DP (^{1}H NMR spectra of macroCTAs are shown in Fig. S1†). The DPs of PVBTMAC macroCTAs from the end group analysis are 24, 50 and 61, which are close to the theoretical ones. A shift in the retention volume distributions agree with the increasing molar mass of

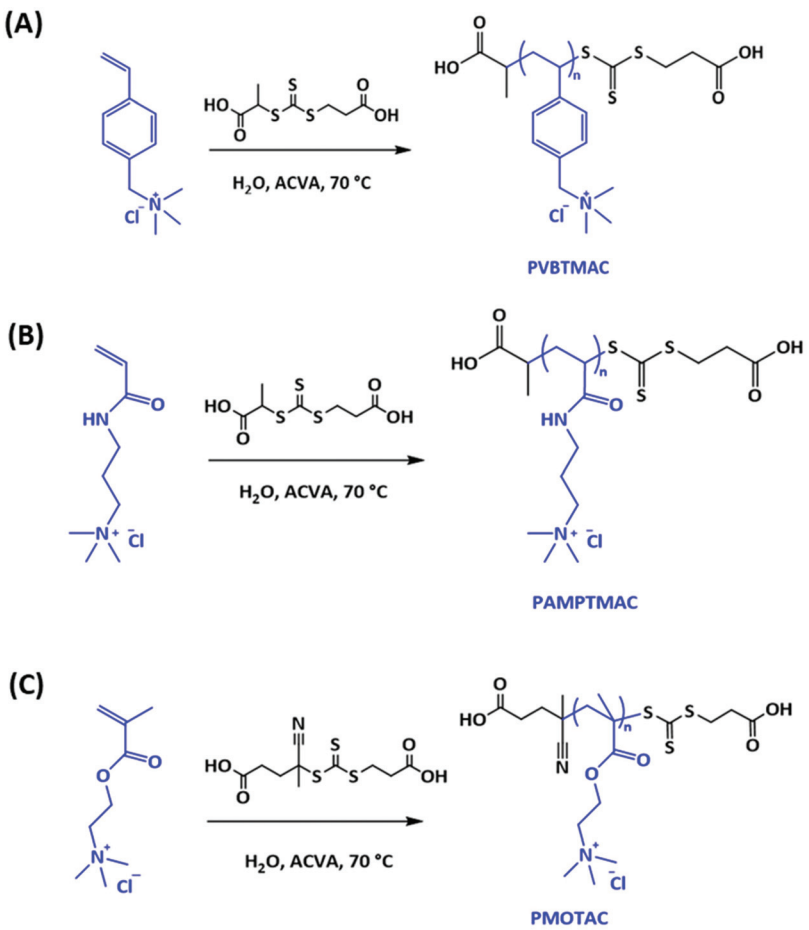

Scheme 1 Syntheses of polycation macroCTAs *via* RAFT polymerization; (A) PVBTMAC, (B) PAMPTMAC and (C) PMOTAC.

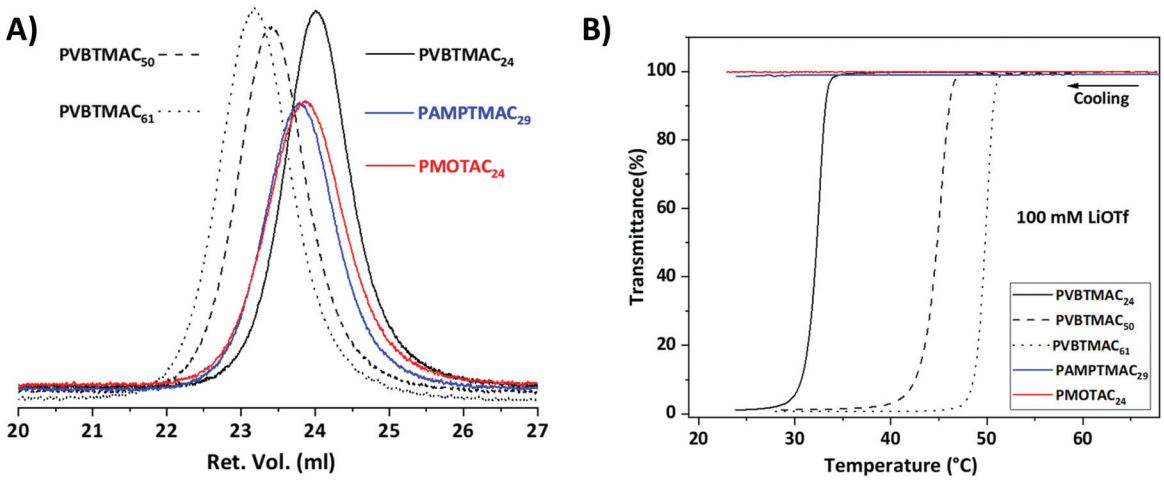

Fig. 1 (A) SEC eluograms of polycation macroCTAs in water/acetonitrile (60/40) with 0.1% trifluoroacetic acid as an eluent. (B) Transmittance cooling curves for polycation macroCTAs (1 mg mL^{-1}) in 100 mM aqueous LiOTf solutions.

macroCTAs. However, broadening of the molar mass distributions with increasing DP of PVBTMAC indicates poor control in the polymerizations. The polydispersity indices of the polymers are shown in Table 1, see also SEC eluograms in Fig. 1A. Broad molar mass distributions were also observed in the other two macroCTAs synthesized with target DP 30. We assume strong charge repulsions along the polymer backbone might have led to either a poor control of polymerizations or a poor separation in SEC.[53] The final DPs and molar masses from NMR were used when conducting the dispersion polymerizations of DAAM.

UCST type phase separation of macroCTAs in triflate solutions

Solution properties of polycation macroCTAs were studied in aqueous triflate solutions. In the presence of hydrophobic triflates, the polycations with aromatic functionalities phase separated upon cooling. However, other macroCTAs PAMPTMAC and PMOTAC were well soluble at all temperatures in 100 mM LiOTf. Styrenic CTA differs from the other two owing to its hydrophobicity, which is in agreement with previous studies on chemically different polycations.[44] Behavior of PVBTMAC is strongly dependent on the molar mass. With increasing the DP, the cloud points shifted to higher temperatures when salt concentration was kept constant (Fig. 1B). Based on these observations we consider the styrenic polycation PVBTMAC more hydrophobic than the methacrylate or acrylamide ones.

Dispersion polymerization of DAAM

The first series of polymerizations of DAAM (the 'NaCl series') were conducted in aqueous solutions using five different polycation macroCTAs (Table S1†). Three of these were styrenic ones with DPs 24, 50, and 61. The DPs of acrylamide and methacrylate CTAs were 29 and 24, respectively. The salt concentration was varied while keeping the solids content constant, 15 w/w%, and target DP of PDAAM 500. The abbreviation V_{24}-D_{500} shows the DP of the CTA (24) and that of PDAAM (500). V stands for the styrenic CTA, M for the methacrylate, and A for acrylamide. Within 3 hours of reaction time, over 98% monomer conversions were achieved in almost every case. Polymerizations conducted with $PVBTMAC_{50}$ showed low monomer conversions at high salt concentrations, see Table S1.† Due to the poor solubility in most solvents, diblock copolymers could not be characterized with SEC. Even the attempts to measure the polymers in methanol and various salts fail because of the adsorption of the polymers to the stationary phase. The problem has often been encountered in PISA investigations.[20,22] With increasing the salt concentration, the turbidities of the dispersions increased. At high salt concentrations, V_{24}-D_{500} dispersions are highly viscous fluids, different from the low viscosity dispersions obtained with other macroCTAs. Similar turbid dispersions were obtained at high solids content 20 w/w%, fluid gel dispersions formed for V_{24}-D_{500} at ionic ratio [NaCl]/[Cp] 12 (Table S2†).

In the latter series, the polymerizations were done in aqueous LiOTf solutions (the 'OTf series'). With either increasing the ionic ratio [LiOTf]/[Cp], [moles of salt per polycation repeating unit] or the molar mass of PVBTMAC, reaction mixtures turned heterogeneous at room temperature. At 70 °C the turbid mixtures became transparent as the solubility of the polycations increased. The self-assembling of the polymers was observed after 30 minutes, when the reaction mixtures turned cloudy again. Later, with increasing degrees of polymerization the systems with high salt concentrations phase separated at 70 °C. Poor DAAM conversions were observed in the polymerizations conducted at high [LiOTf], see Table S3.†

Polymerization kinetics of DAAM were studied using different macroCTAs in aqueous salt (1 M NaCl) solutions, targeting to DP 500 at 15 w/w% solids. As is shown in Fig. 2A the conversion of DAAM rapidly increased during the first 30 min. In all cases, high monomer conversions of DAAM were

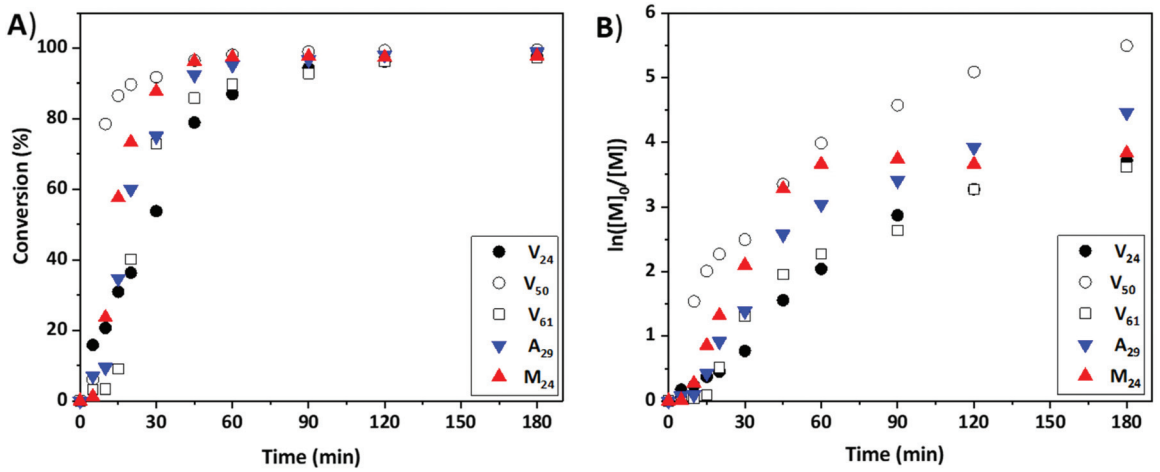

Fig. 2 Kinetics of RAFT dispersion polymerization of DAAM using various macro-CTAs. (A) Conversion of DAAM *versus* time and (B) corresponding semi logarithmic plots.

achieved within 2 h (>97%) as determined by ^{1}H NMR spectroscopy. The corresponding semi logarithmic plot (Fig. 2B) shows the rate of polymerization increased linearly after a 15 minutes induction period. Then, after 60 minutes the increase turned minimal as the monomer concertation decreased. Overall, the rate of polymerizations followed typical reaction kinetics for PISA conducted *via* RAFT dispersion polymerizations.[22,38,52] The ^{1}H NMR spectra of the block copolymers obtained with different macroCTAs are shown in Fig. S2.†

Particles from the NaCl series: morphologies at various ionic ratios

The intensity averaged hydrodynamic diameters and size distributions collected for the dispersions of the NaCl series are plotted in Fig. 3 and summarized in Table S1.† In V_{24}-D_{500} dispersions, hydrodynamic diameters of the particles increased with increasing the ionic ratio from 0 to 16. At ionic ratio 20, a drastic increase of the particle sizes up to 400 nm indicated a morphological transition (Fig. 3f). Interestingly, the polymers

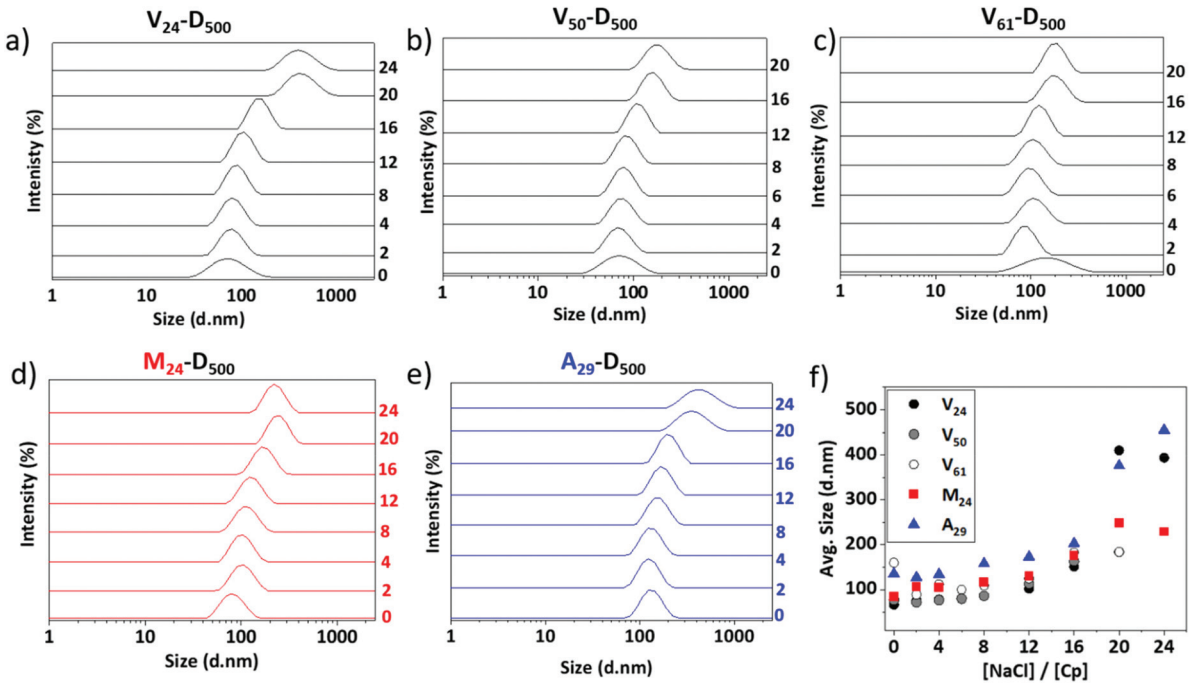

Fig. 3 The size distribution of the dispersions obtained from the NaCl series with varying ionic ratio, (a) V_{24}-D_{500}, (b) V_{50}-D_{500}, (c) V_{61}-D_{500}, (d) M_{24}-D_{500}, (e) A_{29}-D_{500}. The ionic ratio [NaCl]/[Cp] is indicated for each curve on the right axis. (f) Intensity averaged hydrodynamic diameters of the particles. *[Cp] = [polycation repeating unit].

prepared with the acrylamide macroCTA, A_{29}-D_{500} followed the same trends as V_{24}-D_{500}. The styrenic macroCTAs with higher DPs, 50 and 61 produced copolymer particles, the sizes of which increased moderately without showing any indications of morphological changes. The particle diameters were limited to 200 nm in high salt concentrations. The copolymers obtained using the methacrylate CTA, M_{24}-D_{500} behaved in a way very similar to the ones with a long styrenic block.

As is typical in PISA, only spherical particles were obtained from the salt-free dispersions using any of the cationic macroCTAs. When screening the charge density with salt, the reactions led to dispersions with various morphologies. As the polyelectrolytes shrink with ionic screening, efficient chain packing can be expected to allow the fusion of the particles. The morphological phase diagram for the particles is shown in Fig. 4. With short styrenic stabilizers, a clear morphological transition from spheres to fused spheres or aggregated ones and to vesicles took place with increasing the ionic ratio. These observations partially confirm our previous findings, where the morphological transition from spheres to worms to vesicles occurred with increasing salt.[52] In that case, however, the targeting DP of PDAAM was around 250 and the solids content was high, 20 w/w%. The spherical particles were obtained with ionic ratio up to 12 (Fig. 4a and S3a–d†). When the ionic ratio was increased up to 16 the particles consisted of few fused spheres and they looked like cloudberries under TEM (Fig. S3e†). While keeping the ionic ratio 20, the particle morphologies in V_{24}-D_{500} dispersions evolved to vesicle structures (Fig. 4d). Similar morphological changes from spheres to berries occurred either using long styrene based stabilizers or the $PMOTAC_{24}$ macroCTA (Fig. 4 and Fig. S4–6†). On the other hand, V_{50}-D_{500}, V_{61}-D_{500} and M_{24}-D_{500} dispersions (at ionic ratio 20) built up raspberry-like structures, however, no vesicles were observed (see Fig. 4e, f and j).

Chain extension of PAMPTMAC with DAAM at any ionic ratio led to particles with different sizes. Small spherical particles around 20 nm were present in all dispersions (see Fig. 4g, h and S7†). At ionic ratio 16 or below, bigger spherical particles were visible, which were composed of small ones. On the other hand, when increasing the ionic ratio the particles

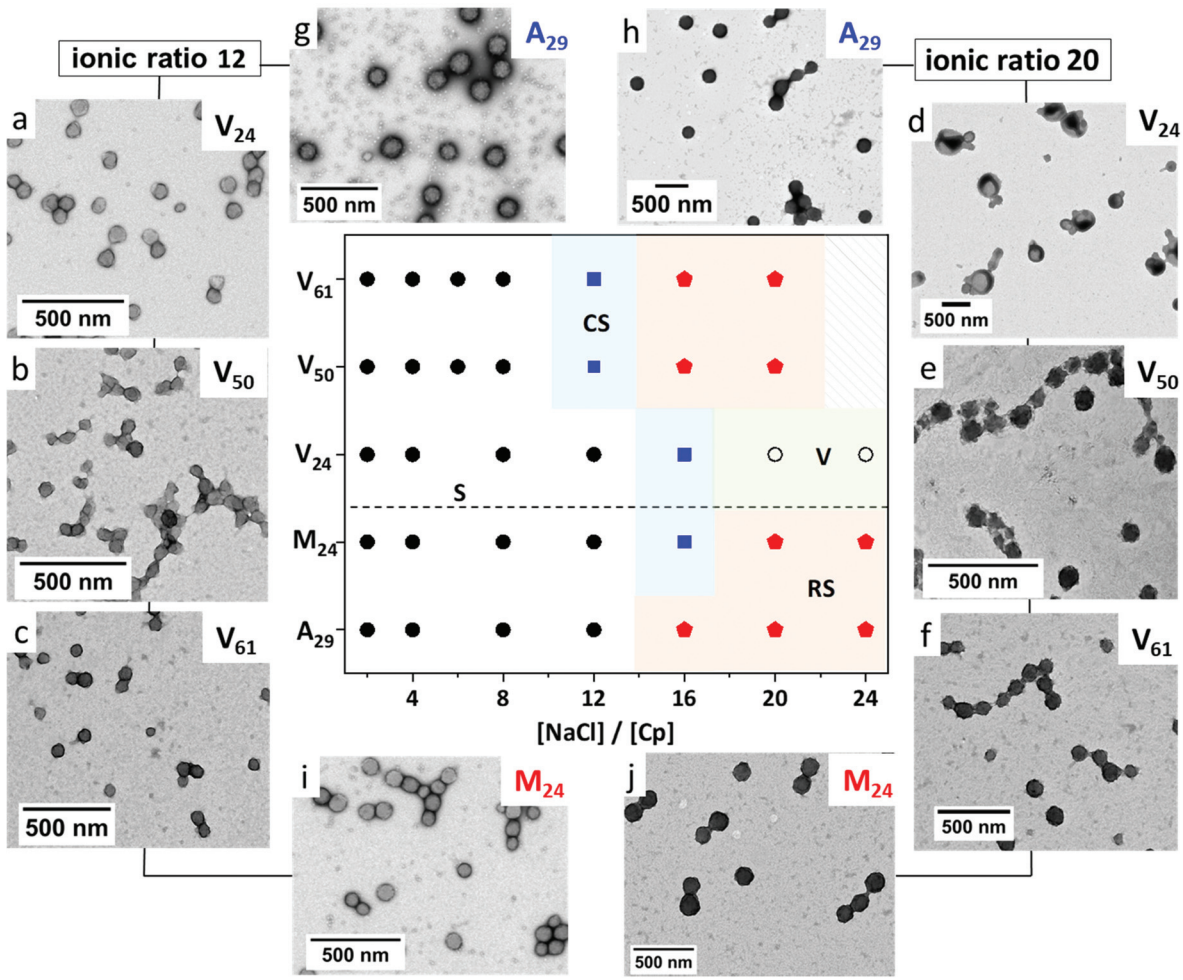

Fig. 4 TEM images of the particles obtained from the NaCl series. (a and d) V_{24}-D_{500}, (b and e) V_{50}-D_{500}, (c and f) V_{61}-D_{500}, (g and h) A_{29}-D_{500}, (i and j) M_{24}-D_{500}. The phase diagram of the particle morphologies at various ionic ratios. S = spheres (●), CS = cloudberry structures (■) RS = raspberry structures (◙) and V = vesicles (○).

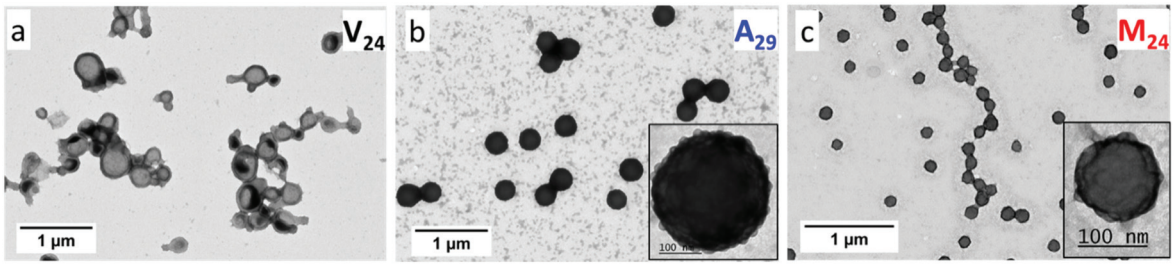

Fig. 5 TEM images of the particles obtained at 15 w/w% using high ionic ratio [NaCl]/[Cp] = 24. Target DP was 500. Details are given in the text.

started to look like raspberries (Fig. 4h). Distinguishing between cloudberries and raspberries was done based on the TEM analysis. The cloudberry particles consist of a low number of fused spheres. In the raspberries, the number of spheres is higher but the spheres are smaller than those in the cloudberries (see enlarged TEM images Fig. S3e and S5e†).

The diameters of the particles measured from TEM images are shown in Fig. S8.† In the dry state, the particle diameters were slightly smaller than those obtained from the DLS (Fig. 3f). In high salt range, the diameters of the A_{29}-D_{500} particles from TEM are almost half of those obtained from DLS. Either this is due to the aggregation in the dispersions or to the hydrophilic nature of acrylamide-based polycation stabilizers. Long hydrophilic grafts on particle surfaces may affect the values obtained with DLS in water.

Fig. 5 shows TEM micrographs of the particles obtained at ionic ratio 24 with three chemically different macroCTAs. With short styrenic macroCTA, vesicles were obtained (Fig. 5a). When the acrylamide based CTA was used, the particles were dense raspberry-like ones (Fig. 5b). Similar morphologies (raspberries) but smaller in size built up when using methacrylate based macroCTA (Fig. 5c).

Increasing the solids content should favor the aggregation processes. Thus, the next experiments were done at 20 w/w% solids using low ionic ratios, either 6 or 12 (Table S2†). Cloudberry-like aggregated structures were obtained with styrene and/or methacrylate based macroCTAs at a low ionic ratio 6 (see Fig. 6a–c). A mixed phase of worms, lamella and vesicles was obtained with increasing the ionic ratio to 12 in the case of V_{24}-D_{500} dispersion (Fig. 6e), corroborating our earlier findings. In the previous paper we have additionally shown that also pure worm and/or vesicle phases may exist with varying salt concentrations.[52] Importantly, with a longer styrenic CTA (DP 50, ionic ratio 12), the particles were berry-like (Fig. 6f). The copolymers obtained with methacrylate or acrylamide CTAs formed mainly raspberry-like structures, see Fig. 6.

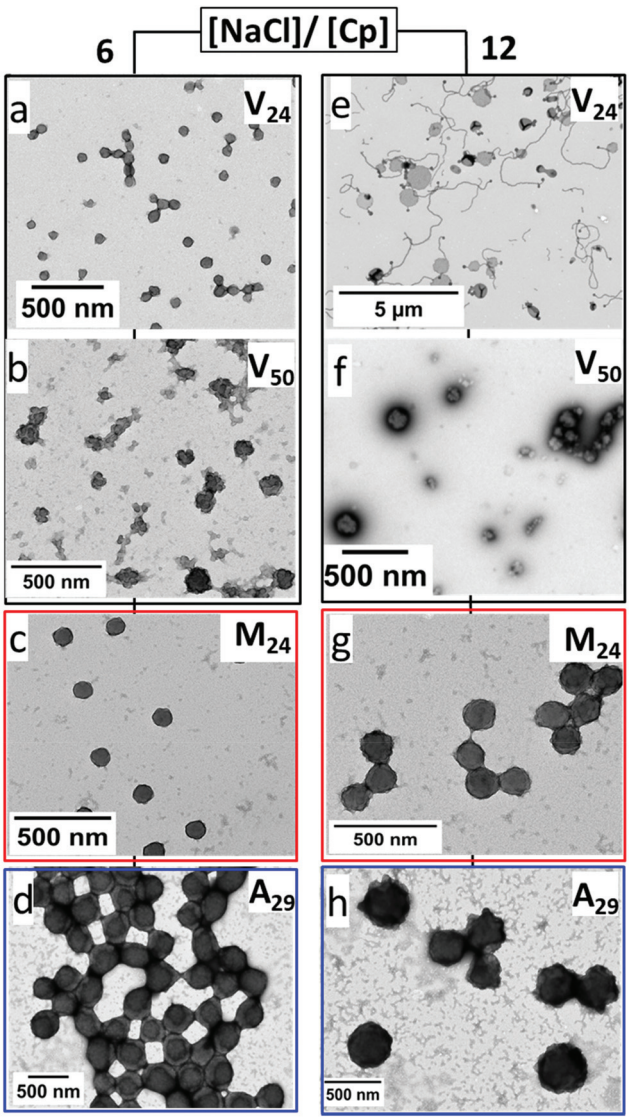

Fig. 6 TEM images of the particles obtained at 20 w/w% using ionic ratios [NaCl]/[Cp] 6 and 12. DP of PDAAM was 500. Details are given in the text.

Morphological transition with triflate ions and temperature (the OTf series)

Based on solution properties of the polycations discussed above, we expected that with triflate ions one could easily quench the charges in the polycation corona. Therefore, the final series of polymerizations was conducted in aqueous triflate solutions. The LiOTf concentration was adjusted respective to the polycation repeating units. The ionic ratio [LiOTf]/[Cp] and solids content were varied while keeping a constant target DP of PDAAM 500. Fig. 7 shows the TEM

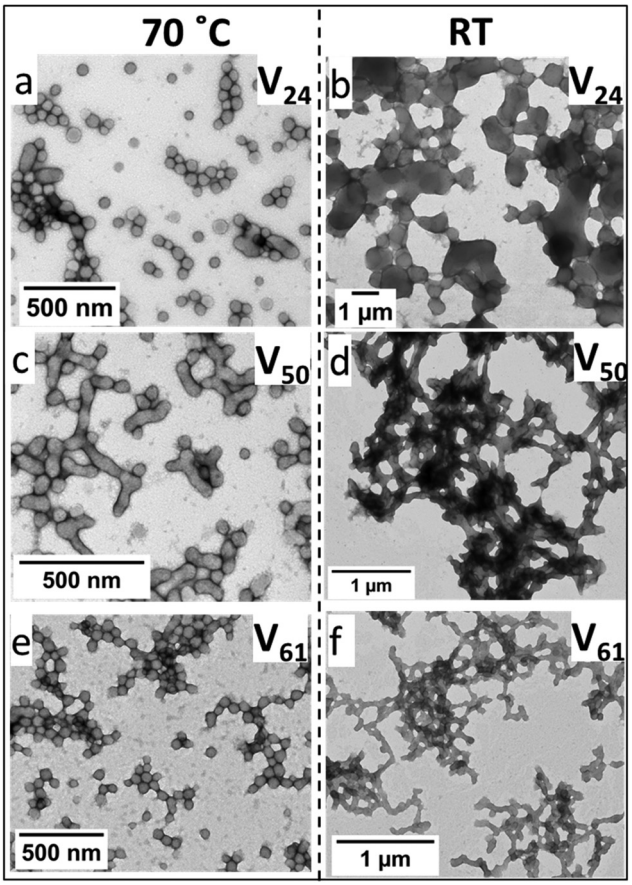

Fig. 7 TEM micrographs of the particles from V_n-D_{500} dispersions obtained in LiOTf solutions at 15 w/w% with ionic ratio [LiOTf]/[Cp] = 1. TEM samples were collected from both hot (from 70 °C, left) and cooled (at room temperature, right) dispersions. See text for details.

images of particles obtained at 15% solids content. The size distributions of the particles from hot solutions are shown in Fig. S9c.† Using ionic ratio [LiOTf]/[Cp] = 1, the copolymers V_{24}-D_{500} self-assembled in to mixtures of spheres and fused spheres at elevated temperature. Upon cooling, the spherical particles aggregated (Fig. 7a and b). For the TEM measurements, the samples were first diluted either at elevated or at room temperature and then applied on the grids. Temperatures of the heated samples certainly change during the application process, however, in such dilute systems morphological transitions are improbable.[38] Interestingly, V_{50}-D_{500} formed fused spheres, whereas the copolymers obtained with longer styrenic stabilizers produced only spherical particles at 70 °C (Fig. 7c and e). Wormlike network structures appeared at room temperature as the polycation coronas underwent phase separation upon cooling (Fig. 7d and f). Several copolymer systems have been shown to undergo morphological transitions (order–order transitions) with changing temperature. Very often, hours or days are needed to allow the transitions to fully take place.[28,29,54,55] In the present case, however, we were following the UCST transition, which was fast and correspondingly, the morphological changes in concentrated samples were instantaneous. With ionic ratios higher than 1, the particles with styrenic blocks precipitated at 70 °C. Thus, the experiments were limited to the ratio 1.

The other polycation stabilizers, PMOTAC and PAMPTMAC, are considered to be more hydrophilic than the styrenic one in the presence of the triflate ions. Consequently, in the dispersions of A_{29}-D_{500} and M_{24}-D_{500} only spherical particles existed at elevated temperatures (Fig. S9a and b†). No morphological transitions took place upon cooling. The findings are important and support the hypothesis that the solubility of the polycation is an essential parameter in PISA, tuning the morphological transitions.

The dispersions of V_{24}-D_{500} turned out to be very sensitive to the solids content. With 17 w/w% solids spherical particles were seen, which aggregated upon cooling (Fig. S10†). With a slightly higher solids content, 20% (ionic ratio kept at 1), a mixture of vesicles and spheres was obtained (Fig. 8a). The vesicles contained small lumens, indicating the membrane had grown inwards to the particles (inset Fig. 8a). The inwards grown vesicles have been observed in nonionic copolymer

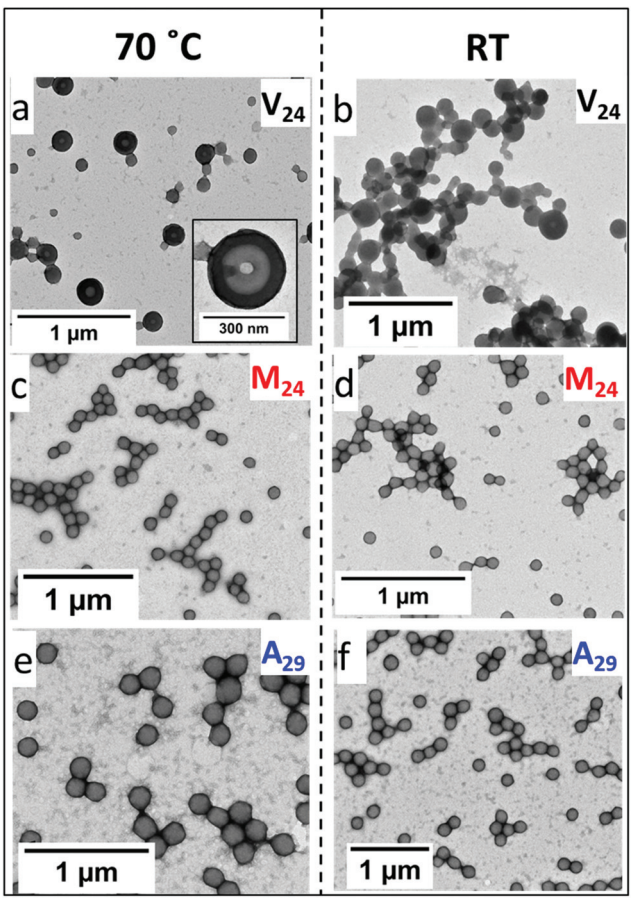

Fig. 8 TEM micrographs of the particles obtained in LiOTf solutions with ionic ratio [LiOTf]/[Cp] = 1 at 20 w/w%. DP of PDAAM was 500. The samples were collected from both hot (70 °C, left) and cooled (room temperature, right) dispersions. More details in the text.

systems where the core-forming block is thermoresponsive.[56–58] Cooling the dispersions led to interconnected vesicles (Fig. 8b).

In the case of longer styrenic polycations, the particles from hot dispersions were fused spheres similar to those shown in Fig. 7; TEM images are shown in ESI (Fig. S11†). Upon cooling, the polymers completely precipitated as the cationic stabilizers lost their solubility. At elevated temperatures, the dispersions obtained from M_{24}-D_{500} and A_{29}-D_{500} at 20 w/w% consisted only of kinetically trapped spheres. Because triflate ions do not change the solubilities of polymethacrylates or polyacrylamides, only spheres existed also at room temperature (Fig. 8c and d for M_{24}-D_{500}, e and f for A_{29}-D_{500}).

Conclusions

Three types of chemically different cationic macroCTAs (methacrylate, acrylamide, styrene) with varying molar masses were synthesized with RAFT. The macroCTAs were chain extended with a hydrophobic core forming monomer DAAM in aqueous solutions with changing the NaCl and total solids concentrations. Only spherical particles were obtained in pure water. However, the morphological transition from spheres to fused spheres or cloudberry-like structures to vesicles was observed with increasing the ionic ratio in case of short styrene based polycation stabilizers V_{24}-D_{500}. Either using long styrene based polycations or the better soluble methacrylate and acrylamide polycations, particle morphologies changed from spheres to cloudberry to raspberry-like structures. At high solids, the polymers with short styrenic cation blocks formed mixed phases; the ones with more soluble polycations were not affected by the solids content.

Next, polymerizations were conducted in aqueous LiOTf solutions at 70 °C. Using ionic ratio [LiOTf]/[Cp] 1, fused spherical structures were obtained in the dispersions of V_n-D_{500}. Upon cooling to room temperature, the V_n-D_{500} particles fused together or even built worm-like networks. Increasing the solids content, the particle morphology changed to vesicles in case of the short styrenic CTA, V_{24}-D_{500}. The morphological changes were mainly due to the changing solubility of the styrenic polycations in the presence of LiOTf. In the case of more hydrophilic macroCTAs, no changes in the morphologies were observed.

To sum up, we have shown that particles with various morphologies can be obtained using sole polycation stabilizers by screening the charges in the coronas with NaCl. With hydrophobic counterions like triflate, morphological changes can be induced even with a low ionic ratio. Because the triflate ions turn the styrenic polycations thermoresponsive, one can tune the morphologies also with temperature.

Conflicts of interest

There are no conflict to declare.

Acknowledgements

Electron Microscopy Unit of the Institute of Biotechnology, University of Helsinki, is acknowledged for providing the microscopy facilities. VB thanks Magnus Ehrnrooth Foundation for the research grant.

Notes and references

1 C. J. Ferguson, R. J. Hughes, B. T. T. Pham, B. S. Hawkett, R. G. Gilbert, A. K. Serelis and C. H. Such, *Macromolecules*, 2002, **35**, 9243–9245.
2 C. J. Ferguson, R. J. Hughes, D. Nguyen, B. T. T. Pham, R. G. Gilbert, A. K. Serelis, C. H. Such and B. S. Hawkett, *Macromolecules*, 2005, **38**, 2191–2204.
3 S. Y. Khor, N. P. Truong, J. F. Quinn, M. R. Whittaker and T. P. Davis, *ACS Macro Lett.*, 2017, **6**, 1013–1019.
4 X. Zhang, J. Rieger and B. Charleux, *Polym. Chem.*, 2012, **3**, 1502–1509.
5 A. Blanazs, A. J. Ryan and S. P. Armes, *Macromolecules*, 2012, **45**, 5099–5107.
6 S. Boissé, J. Rieger, G. Pembouong, P. Beaunier and B. Charleux, *J. Polym. Sci., Part A: Polym. Chem.*, 2011, **49**, 3346–3354.
7 W. Zhang, F. D'Agosto, O. Boyron, J. Rieger and B. Charleux, *Macromolecules*, 2012, **45**, 4075–4084.
8 D. Zhou, S. Dong, R. P. Kuchel, S. Perrier and P. B. Zetterlund, *Polym. Chem.*, 2017, **8**, 3082–3089.
9 J. Rieger, F. Stoffelbach, C. Bui, D. Alaimo, C. Jérôme and B. Charleux, *Macromolecules*, 2008, **41**, 4065–4068.
10 B. Charleux, G. Delaittre, J. Rieger and F. D'Agosto, *Macromolecules*, 2012, **45**, 6753–6765.
11 X. Zhang, S. Boissé, W. Zhang, P. Beaunier, F. D'Agosto, J. Rieger and B. Charleux, *Macromolecules*, 2011, **44**, 4149–4158.
12 Y. Li and S. P. Armes, *Angew. Chem., Int. Ed.*, 2010, **49**, 4042–4046.
13 G. Delaittre, C. Dire, J. Rieger, J. L. Putaux and B. Charleux, *Chem. Commun.*, 2009, 2887–2889.
14 S. Sugihara, A. Blanazs, S. P. Armes, A. J. Ryan and A. L. Lewis, *J. Am. Chem. Soc.*, 2011, **133**, 15707–15713.
15 N. J. Warren and S. P. Armes, *J. Am. Chem. Soc.*, 2014, **136**, 10174–10185.
16 N. J. W. Penfold, J. Yeow, C. Boyer and S. P. Armes, *ACS Macro Lett.*, 2019, **8**, 1029–1054.
17 M. Semsarilar, V. Ladmiral, A. Blanazs and S. P. Armes, *Langmuir*, 2012, **28**, 914–922.
18 M. Williams, N. J. W. Penfold and S. P. Armes, *Polym. Chem.*, 2016, **7**, 384–393.
19 L. Zhang, R. J. Barlow and A. Eisenberg, *Macromolecules*, 1995, **28**, 6055–6066.
20 M. Semsarilar, V. Ladmiral, A. Blanazs and S. P. Armes, *Langmuir*, 2013, **29**, 7416–7424.

21 M. Williams, N. J. W. Penfold, J. R. Lovett, N. J. Warren, C. W. I. Douglas, N. Doroshenko, P. Verstraete, J. Smets and S. P. Armes, *Polym. Chem.*, 2016, **7**, 3864–3873.
22 S. J. Byard, A. Blanazs, J. F. Miller and S. P. Armes, *Langmuir*, 2019, **35**, 14348–14357.
23 B. Zhang, X. Yan, P. Alcouffe, A. Charlot, E. Fleury and J. Bernard, *ACS Macro Lett.*, 2015, **4**, 1008–1011.
24 D. Cordella, F. Ouhib, A. Aqil, T. Defize, C. Jérôme, A. Serghei, E. Drockenmuller, K. Aissou, D. Taton and C. Detrembleur, *ACS Macro Lett.*, 2017, **6**, 121–126.
25 J. Demarteau, A. Fernandez De Anãstro, A. S. Shaplov and D. Mecerreyes, *Polym. Chem.*, 2020, **11**, 1481–1488.
26 D. Cordella, A. Debuigne, C. Jérôme, Z. Kochovski, D. Taton and C. Detrembleur, *Macromol. Rapid Commun.*, 2016, 1–7.
27 A. Blanazs, R. Verber, O. O. Mykhaylyk, A. J. Ryan, J. Z. Heath, C. W. I. Douglas and S. P. Armes, *J. Am. Chem. Soc.*, 2012, **134**, 9741–9748.
28 K. Doncom, N. J. Warren and S. P. Armes, *Polym. Chem.*, 2015, **6**, 7264–7273.
29 J. R. Lovett, N. J. Warren, S. P. Armes, M. J. Smallridge and R. B. Cracknell, *Macromolecules*, 2016, **49**, 1016–1025.
30 N. J. W. Penfold, J. R. Whatley and S. P. Armes, *Macromolecules*, 2019, **52**, 1653–1662.
31 D. L. Beattie, O. O. Mykhaylyk, A. J. Ryan and S. P. Armes, *Soft Matter*, 2021, **17**, 5602–5612.
32 R. Verber, A. Blanazs and S. P. Armes, *Soft Matter*, 2012, **8**, 9915–9922.
33 Y. Pei, A. B. Lowe, P. J. Roth, Y. Pei, P. J. Roth and A. B. Lowe, *Macromol. Rapid Commun.*, 2017, **38**, 1600528.
34 L. P. D. Ratcliffe, M. J. Derry, A. Ianiro, R. Tuinier and S. P. Armes, *Angew. Chem.*, 2019, **131**, 19140–19146.
35 K. E. B. Doncom, N. J. Warren and S. P. Armes, *Polym. Chem.*, 2015, **6**, 7264–7273.
36 N. J. Warren, M. J. Derry, O. O. Mykhaylyk, J. R. Lovett, L. P. D. Ratcliffe, V. Ladmiral, A. Blanazs, L. A. Fielding and S. P. Armes, *Macromolecules*, 2018, **51**, 8357–8371.
37 J. R. Lovett, N. J. Warren, L. P. D. Ratcliffe, M. K. Kocik and S. P. Armes, *Angew. Chem., Int. Ed.*, 2015, **54**, 1279–1283.
38 S. J. Byard, M. Williams, B. E. McKenzie, A. Blanazs and S. P. Armes, *Macromolecules*, 2017, **50**, 1482–1493.
39 X. Wang, J. Zhou, X. Lv, B. Zhang and Z. An, *Macromolecules*, 2017, **50**, 7222–7232.
40 S. J. Byard, C. T. O'Brien, M. J. Derry, M. Williams, O. O. Mykhaylyk, A. Blanazs and S. P. Armes, *Chem. Sci.*, 2020, **11**, 396–402.
41 M. J. Derry, O. O. Mykhaylyk and S. P. Armes, *Angew. Chem.*, 2017, **129**, 1772–1776.
42 I. R. Dorsman, M. J. Derry, V. J. Cunningham, S. L. Brown, C. N. Williams and S. P. Armes, *Polym. Chem.*, 2021, **12**, 1224–1235.
43 Y. Pei, N. C. Dharsana, J. A. Van Hensbergen, R. P. Burford, P. J. Roth and A. B. Lowe, *Soft Matter*, 2014, **10**, 5787–5796.
44 E. Karjalainen, V. Aseyev and H. Tenhu, *Macromolecules*, 2014, **47**, 7581–7587.
45 Y. Men, H. Schlaad and J. Yuan, *ACS Macro Lett.*, 2013, **2**, 456–459.
46 Y. Kohno, S. Saita, Y. Men, J. Yuan and H. Ohno, *Polym. Chem.*, 2015, **6**, 2163–2178.
47 V. Baddam, V. Aseyev, S. Hietala, E. Karjalainen and H. Tenhu, *Macromolecules*, 2018, **51**, 9681–9691.
48 H. Yoshimitsu, A. Kanazawa, S. Kanaoka and S. Aoshima, *Macromolecules*, 2012, **45**, 9427–9434.
49 E. Karjalainen, N. Suvarli and H. Tenhu, *Polym. Chem.*, 2020, **11**, 5870–5883.
50 V. Baddam, R. Missonen, S. Hietala and H. Tenhu, *Macromolecules*, 2019, **52**, 6514–6522.
51 E. Karjalainen, V. Aseyev and H. Tenhu, *Polym. Chem.*, 2015, **6**, 3074–3082.
52 V. Baddam, L. Välinen and H. Tenhu, *Macromolecules*, 2021, **54**, 4288–4299.
53 Y. Mitsukami, M. S. Donovan, A. B. Lowe and C. L. McCormick, *Macromolecules*, 2001, **34**, 2248–2256.
54 L. P. D. Ratcliffe, M. J. Derry, A. Ianiro, R. Tuinier and S. P. Armes, *Angew. Chem., Int. Ed.*, 2019, **58**, 18964–18970.
55 L. Hahn, M. Maier, P. Stahlhut, M. Beudert, V. Flegler, S. Forster, A. Altmann, F. Töppke, K. Fischer, S. Seiffert, B. Böttcher, T. Lühmann and R. Luxenhofer, *ACS Appl. Mater. Interfaces*, 2020, **12**, 12445–12456.
56 N. J. Warren, O. O. Mykhaylyk, A. J. Ryan, M. Williams, T. Doussineau, P. Dugourd, R. Antoine, G. Portale and S. P. Armes, *J. Am. Chem. Soc.*, 2015, **137**, 1929–1937.
57 J. Siirilä, S. Häkkinen and H. Tenhu, *Polym. Chem.*, 2019, **10**, 766–775.
58 Q. Zhang, R. Zeng, Y. Zhang, Y. Chen, L. Zhang and J. Tan, *Macromolecules*, 2020, **53**, 8982–8991.